Bachelor Thesis

Degree Project in
Geological Sciences, 15 hp

Shear Zone Investigation Between Two Blueschist Units on Sikinos Island, Southern Cyclades, Greece

Erik Käll

Stockholm 2026

Department of Geological Sciences
Stockholm University
SE-106 91 Stockholm

Contents

Abstract

The aim of this bachelor thesis was to map an area between two unpublished blueschist samples from Sikinos Island in the southern Cyclades, which yielded different ages. The age gap suggests a thrust of the older blueschist unit in the northeast over the younger one in the west. The objective of this bachelor thesis was to investigate whether there is a thrust-type shear zone between these two sample sites, accommodating the displacement.

To investigate the possibility of a shear zone, mapping was carried out. The aim of the mapping was to find a mylonitic zone indicating the existence of a shear zone. This mapping included determining the lithology, measuring structural fabrics (foliation and stretching lineations), determining relative shear sense, and collecting representative samples from sites across the field area. These samples were subsequently cut down to thin sections and investigated structurally and petrographically.

The results of the analysis support the interpretation of a thrust-type shear zone between the two sample locations, but additional geochronological data are needed to constrain the timing of the deformation.

1.Introduction

The southern Cyclades, including the island of Sikinos, are located in the Aegean Sea. This region has a lithology belonging to the Cycladic Blueschist Unit and the Cycladic Basement. These rocks have a complex tectonometamorphic history characterized by high-pressure metamorphism associated with subduction, followed by exhumation.

Compared to its neighbours, the island of Sikinos has received relatively little attention from geologists. Only in recent years has more extensive investigation been conducted on Sikinos tectonic history.

1.2 Objective

The primary objective of this thesis was to investigate the presence of a shear zone between Agios Georgios Bay and Chora on Sikinos Island. The assumption of an existing shear zone was based on unpublished dating of two blueschist samples by Glodny and Ring (Ring, pers.

comm., 2026). Sample SIK 20-8 from Agios Georgios Bay which yielded an age of 38.6 ± 1.3 Ma and sample SIK 20-11, taken south of the road junction near Chora, which yielded an age of 30.4 ± 2.0 Ma (U. Ring personal communication). These new data suggest a thrust of the older blueschist in the northeast over the younger blueschist in the west.

2.Setting

2.1 Hellenides and the southern Cyclades

2.1.1 Hellenides

The Hellenides is an arcuate orogen located north of the southward-retreating Hellenic margin, where the African plate is subducted beneath the Eurasian plate and the Aegean microplate (Ring, Glodny and Peillod, 2025). The Hellenides orogen is located in the Mediterranean Sea and stretches from the mainland of Greece across the Aegean Sea through Crete to western Turkey (see Fig. 1).

The earliest evidence of high-pressure (high-P) metamorphism in the Hellenides orogeny started in the northern Cyclades at ∼53 Mya, related to Hellenic slab subduction (Ring et al., 2010). The oldest high-P rocks formed in the northern part of the Aegean transect, and progressively younger high-P rocks formed towards the south)(Jolivet and Brun, 2010; Ring and Glodny, 2021). This progressive younging in age reflects the southward retreat of the Hellenic subduction slab (Jolivet *et al.*, 2015; Ring and Glodny, 2021).

The Hellenides orogen is divided into different tectonic domains based on the type of rocks, tectonometamorphic history, and stratigraphy (Jolivet and Brun, 2010; Ring *et al.*, 2010). In this study, the focus will be placed on the Pindos oceanic unit, which contains the subunits: Cycladic Blueschist Unit (CBU) (Fig. 1) and the Cycladic Basement Unit, which can be found in the studied field area on Sikinos Island.

2.1.2 The southern Cycladic archipelago

The Cycladic archipelago is made up of 220 islands, with Sikinos located in the southern part of this archipelago (Fig. 1).

One of the tectonic domains in the southern Cyclades is Pindos, with the two subunits: the Cycladic Blueschist Unit (CBU) and the Cycladic Basement Unit (Jolivet and Brun, 2010).

The intermediate Cycladic Blueschist Unit and the Cycladic Basement are the main units on Sikinos (Augier *et al.*, 2015).

Pindos, which contains both the CBU and the Cycladic Basement, underwent a high-pressure (high-P), low-temperature (low-T) metamorphic event around 53–30 Mya (Augier et al., 2015) (Fig. 2). The CBU experienced higher pressure than the Cycladic Basement, reaching blueschist- to eclogite-facies conditions (Ring, Glodny and Peillod, 2025). This high-P event was caused by the underthrusting of the Hellenic slab (Ring *et al.*, 2010). After the high-P event, the CBU and the Cycladic Basement were progressively overprinted by greenschist conditions during exhumation.

The majority of exhumation of Pindos and the CBU occurred in extrusion wedges while lithospheric convergence was still taking place; a second, more limited stage of exhumation occurred during lithospheric extension (Ring et al., 2010; Augier et al., 2015). This extension opened the Aegean Sea basin during pronounced rollback of the subduction zone at 23–19 Mya (Ring *et al.*, 2010; Grasemann *et al.*, 2012) (Fig. 2). In this post-orogenic stage, the CBU and the Cycladic Basement Unit were exhumed as Cordilleran-type metamorphic core complexes (Lister, Banga and Feenstra, 1984; Augier *et al.*, 2015). The extension in the central and northern Cyclades was top-to-the-N directed, and in the southern Cyclades top-to-the-S directed (Bakowsky *et al.*, 2023). Sikinos is situated within the hinge zone separating the two differently directed extensional systems (Ring, Glodny and Peillod, 2025).

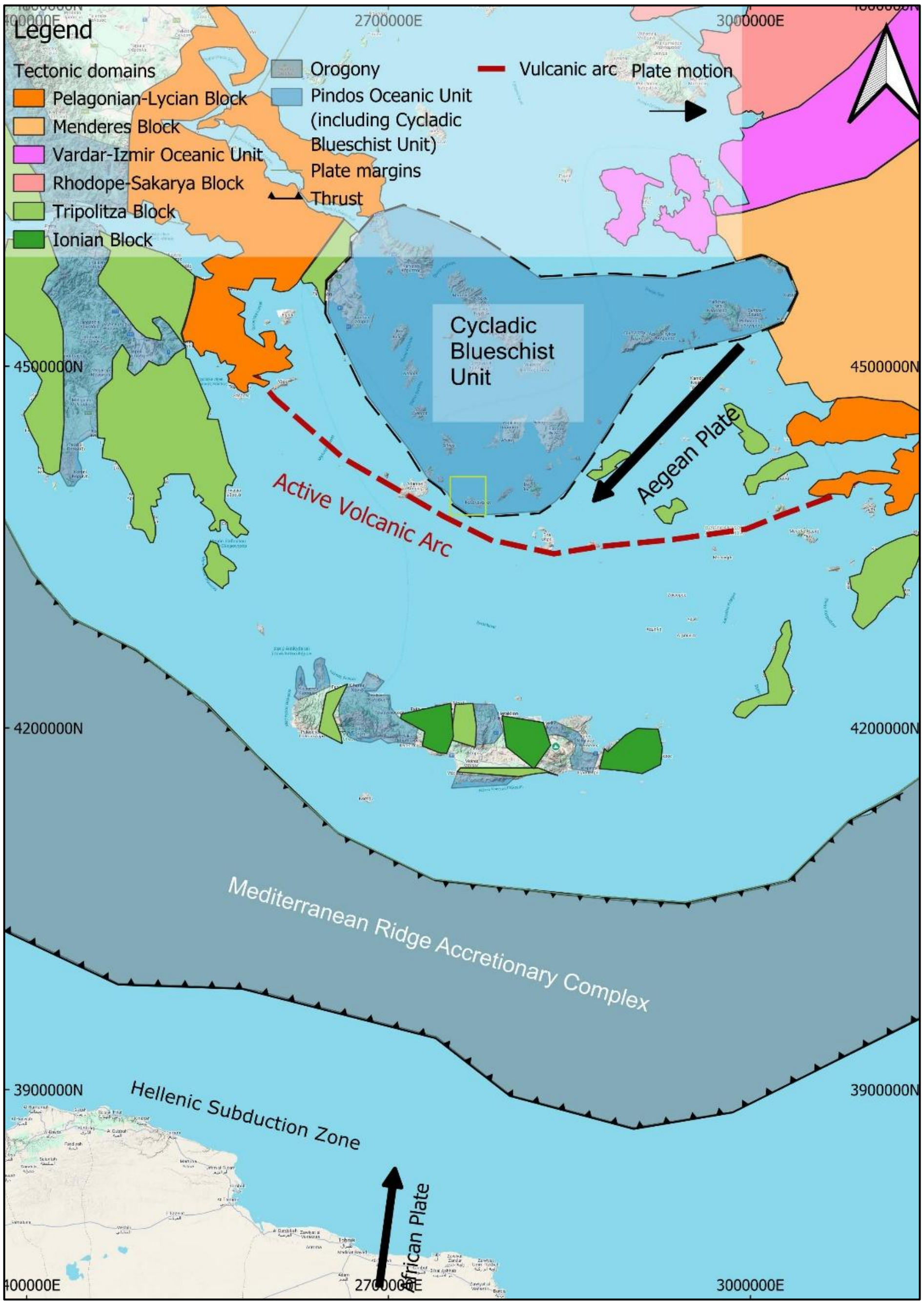

Fig.1 Overview of the Hellenides and Aegean Sea (including the Cycladic archipelago). The map is based on (Ring et al., 2010) and (Meng et al., 2021) . The map shows the location of the retreating Hellenic subduction zone, arrows indicating movement of the plates, the position of CBU and Sikinos, plate margins, the Mediterranean Ridge accretionary complex and the volcanic arc spanning across the Aegean Sea.

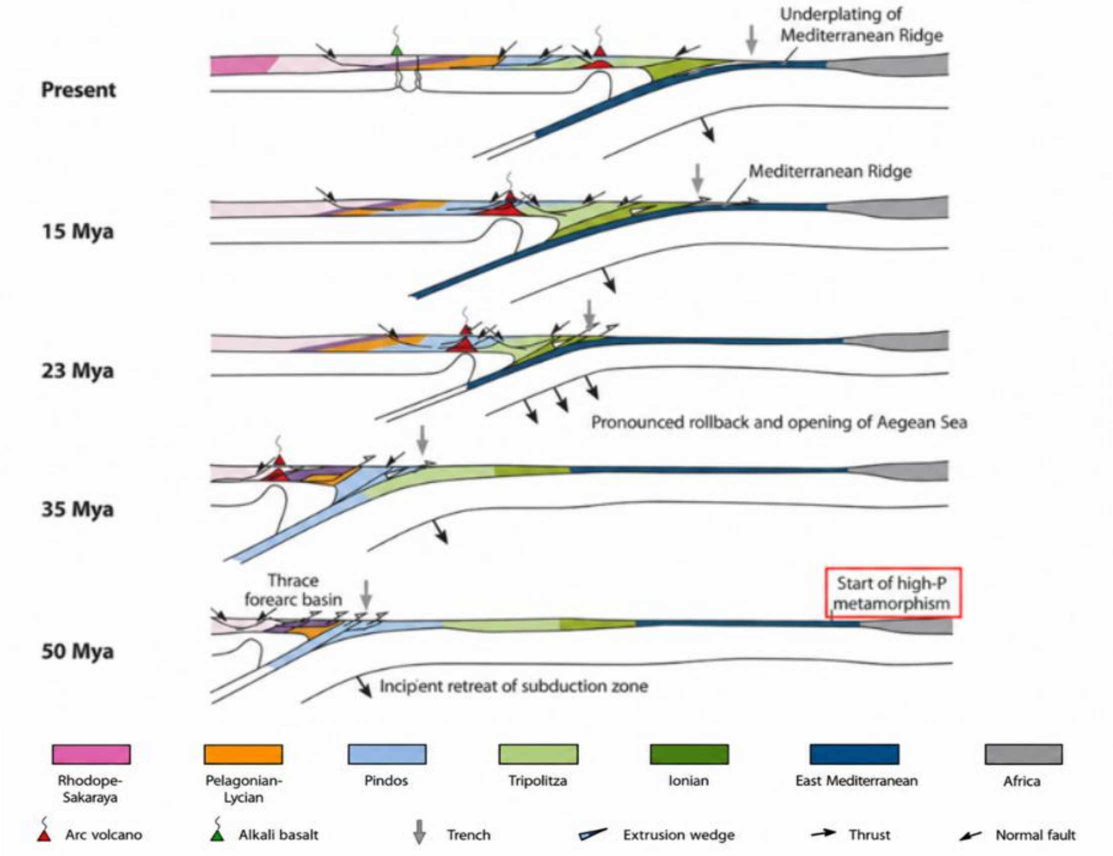

Fig.2 *Modified figure from (Ring et al., 2010) with assistance from ChatGPT, shows the start of the high pressure, low temperature event around 53-30 Mya in which the Pindos (containing the CBU and the Cycladic basement) became subducted and the subsequent overprint in the Miocene at 23 Mya. The figure also shows the how Pindos got exhumed through extrusion wedges and later extension during the opening of the Aegean Sea (related to the pronounced rollback).*

2.2 Geology of Sikinos

Sikinos consists of two tectonometamorphic units: the Cycladic Basement and the tectonically overlying CBU passive-margin sequence (Augier et al., 2015; Ring, Glodny and Peillod, 2025). The basement rocks are composed of granodioritic gneiss, metavolcanics, garnet mica schist, schist, and rare amphibolites (Ring, Glodny and Peillod, 2025). The 6–7 km thick CBU passive-margin sequence is composed of marble layers (dolomitic and calcitic), quartz mica schist, and minor occurrences of metabasite lenses (Fig. 3) (Augier et al., 2015; Ring, Glodny and Peillod, 2025; Polauki, 2019). The metabasite lenses (eclogite, blueschist, and greenschist) provide peak P–T conditions of 16–20 kbar and 480–540 °C. On Sikinos, higher-pressure rocks are preserved between retrograded rocks (Augier et al., 2015). Most of the P–T work on Sikinos has been on mafic rocks (metabasites), but it is understood that the surrounding metapelites underwent the same type of conditions (Glodny and Ring, 2022).

Sikinos, as previously discussed, is located within the hinge zone separating the two differently directed extensional systems. Top-to-the-S shearing was previously thought to be exclusively related to thrusting of the CBU over the Cycladic Basement. This thrust was speculated by Ring and Glodny (2021) to have an age of 35–30 Mya, similar to top-to-the-S thrust observed in the southern parts of the neighbouring island Ios(Huet, Labrousse and Jolivet, 2009). However, recent dating (Ring, Glodny and Peillod, 2025) indicates that top-to-the-S deformation in the Cycladic Basement also reflects extensional deformation at ~23 Ma. This early south-directed extension was subsequently overprinted by north-directed extensional structures (Ring, Glodny and Peillod, 2025).

The top-to-the-S structures on Sikinos did not all form under the same metamorphic grade, with the first top-to-the-S structures forming under blueschist conditions and then progressively overprinted by greenschist conditions during exhumation (Fig. 2) (Ring, Glodny and Peillod, 2025). The shear zones on Sikinos were mainly active under greenschist conditions, and some transitioned to a brittle regime during the final stages of exhumation (Augier et al., 2015).

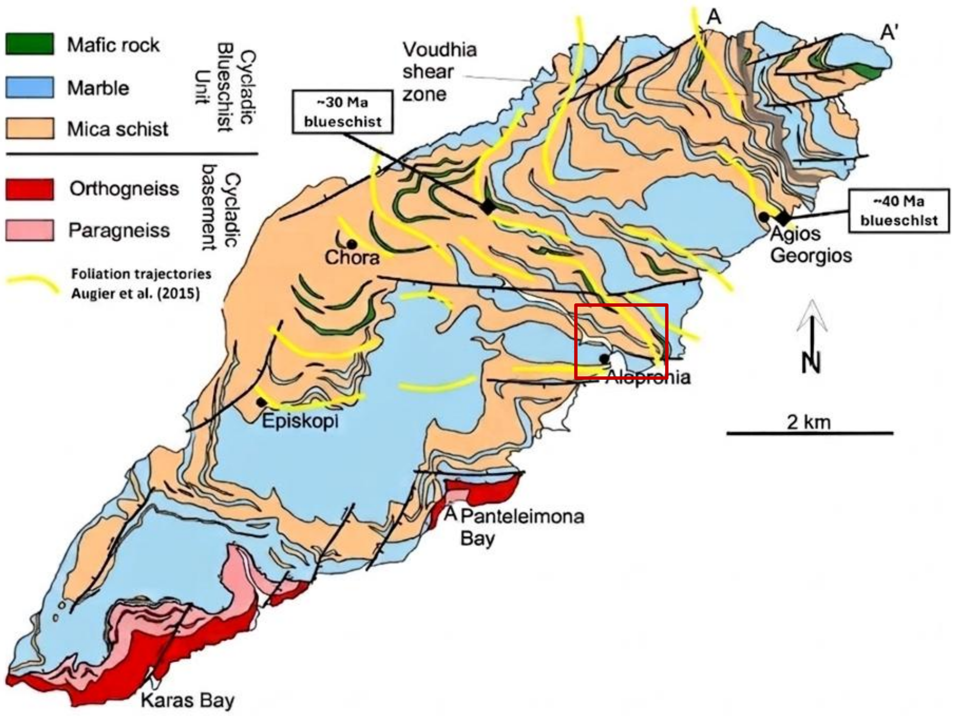

Fig.3 *Geologic map of Sikinos Island, modified from (Ring and Glodny, 2021) and foliation trajectory extracted from (Augier et al., 2015). The red square on the map indicates the field area mapped in this project.*

2.3 Background on shear zones

A shear zone can develop across a wide range of scales and may form under either ductile or brittle conditions. The transition between these regimes depends on several factors, such as fluid pressure, stress orientation, and the geothermal gradient. The ductile regime is characterized by mylonitic textures defined as fine grain size, well-developed foliation, and lineations parallel to the shear direction. In contrast, the brittle regime is characterized by the presence of faults. To determine the sense of shear, kinematic indicators such as shear bands and mantled porphyroclasts are commonly used.(Van der Pluijm and Marshak, 2004)

3. Method

The fieldwork was conducted on the island of Sikinos in April 2026. The primary objective of the project was to investigate the presence of a shear zone. This was done by measuring structural fabrics (foliation and stretching lineations) and lithology, determining relative shear sense, and collecting representative samples from different sites across a mylonitic zone (Fig. 3).

The fieldwork resulted in two data sets:

1. Macroscopic field data: including structural measurements (dip direction and dip of the foliation planes, as well as the trend and plunge of the stretching lineations). Additionally, rock types and mesoscopic shear sense indicators were identified based on macroscopic field observations.

2. Microscopic data observations: thin section data derived from the collected field samples. This dataset contains types of minerals, lithological confirmation, and microscopic shear sense indicators.

3.1 Mapping strategy

The mapping area was defined together with Uwe Ring. We based our choice on (Augier *et al.*, 2015) hypothesis on a small, discontinuous shear zone, combined with unpublished data on two blueschist samples (U. Ring personal communication).

Macroscopic field data was recorded manually in both a field notebook and via **SW maps** (mobile application, which record GPS coordinates, photos and field remarks). If possible, lithological classification, structural measurement, shear sense indicators and GPS coordinates were documented at every stop. Structural measurements were acquired using a **Krantz** compass. Lithology identification was made by macroscopic field observations, with type of rock logged directly into SW maps and an analogue field map. If two rock types were observed at the same location, the dominant rock type was logged.

Subsequently, all field data were transcribed into Excel sheets, which allowed the data to be easier to handle and extracted into specific sub-groups: foliation, stretching lineation, shear sense, rock type and GPS coordinates.

Final mapping and digitization were performed in **QGIS**, with Google Terrain as the base layer. The coordinate reference system used was **WGS 84 / Pseudo-Mercator**. The lithology was digitized based on the rock type observations made in the field.

The foliation and stretching lineations were put into (Stereonet11, Rick Allmendinger) for calculation of foliation planes into poles and analysis of best fitted great circle with Bingham analysis.

3.2 Shear sense indicators

Shear sense indicators can be seen on all scales within a shear zone, spanning from the meter-scale down to microscopic levels. Identifying and assigning the relative shear sense can be a hard task in the field. Many outcrops can be overprinted and contain both top-to-the-south and top-to-the-north shear sense. This gives room for some interpretation in reading the shear sense. On outcrops with bidirectional shear sense, all the observed indicators were counted, and the dominating shear sense was documented. As well as the shear sense the metamorphic facies were documented.

3.3 Thin section analysis

During the fieldwork 4 samples were collected and prepared into thin sections. These were subsequently analysed with the help of microscopes at Stockholms university. Each thin section was examined under both plane polarised light (PPL) and cross polarised light (XPL). Representative parts of the thin section were photographed and documented using, LAS EZ Imaging Software for Windows.

4.Results

From the data collected during mapping four maps of the study area were created: Lithology, Foliation, Lineation and Shear Sense.

4.1 Lithology

In the area in which the study took place, three dominant rock types were identified: marble, mica schist, and metabasites (greenschist and blueschist). Although two types of marble were observed—dolomitic and calcitic—they were grouped together as marble due to limited data and for simplification. The competent marbles make up prominent ridges in the mapping area, where the softer metapelitic rocks usually form the valleys (Fig. 4). Mylonitic texture was found in all lithologies but was most abundant in the schists. At the contact between schist and marble, strong stretching is evident in the marble, expressed as boudinage structures (Fig. 5). In the valley and on top of the prominent ridges, the marble appears relatively undeformed.

Mica schist is found to the west of the western prominent ridge and stretches through the central region of the field area (Fig. 4). Two main types of mica schist were distinguished: garnet mica schist (Fig. 5) and quartz mica schist (Fig. 6). The garnet mica schist was only found at two locations, Dialiskari Beach and a small outcrop inside the greenschist lens. All mica schist found showed mylonitic texture, characterized by small grain size. Only in the north-central part of the study area was a transition from ductile to brittle regime identified, where mylonitic textures were overprinted by brittle deformation.

Metabasites occur in lenses, primarily around Dialiskari Beach and in the area northeast of the beach (Fig. 4). These metabasites include both greenschist and blueschist, often imbricated together at the locations of measurement (Fig. 5).

At Dialiskari Beach, a continuous rock sequence was identified, with blueschist and garnet-bearing mica schist at the base. Above this, greenschist imbricated with blueschist was observed. Overlying the greenschist is quartz–mica schist, followed by marble at the top (Fig. 5).

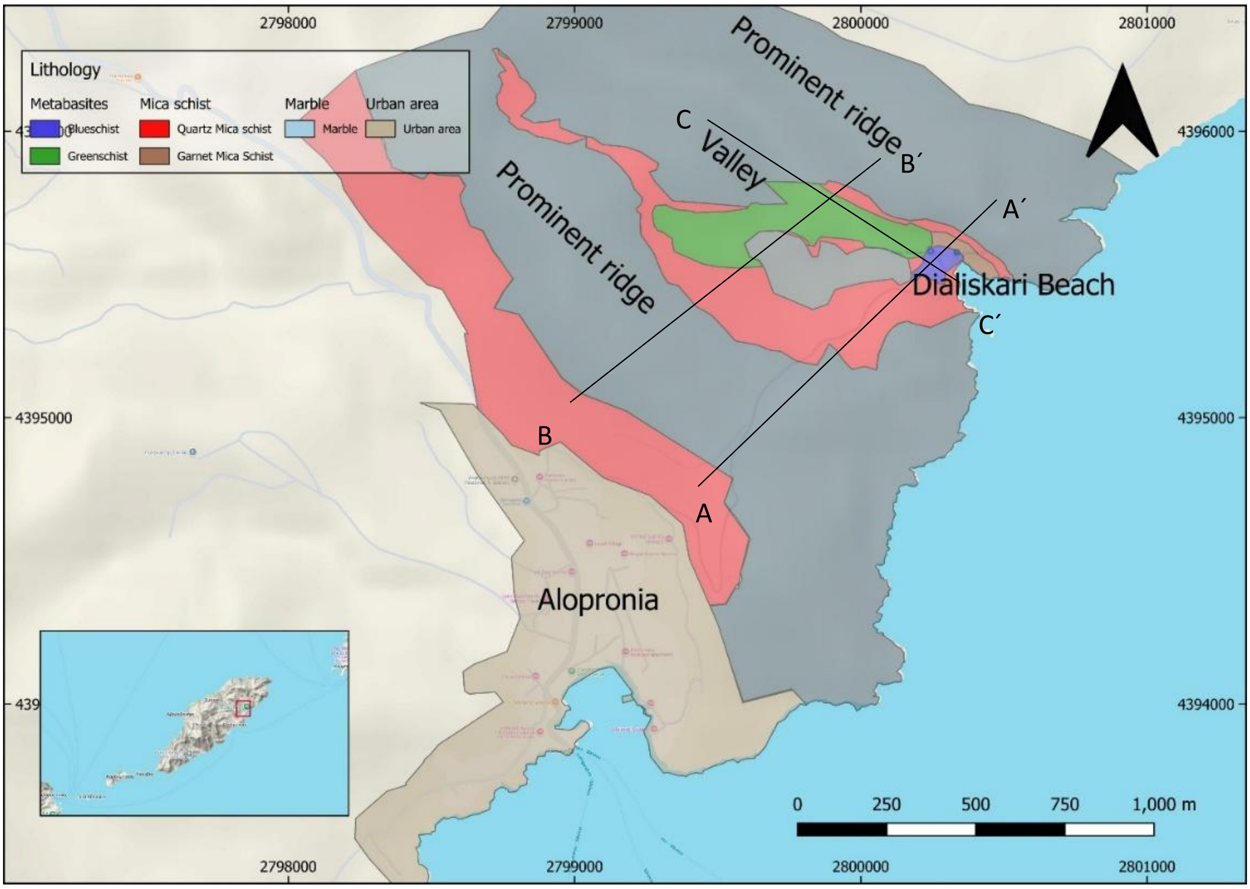

Fig.4 *Geological map of Dialiskari Beach and Alopronia showing the three cross sections (A–A', B–B', and C–C'). The map illustrates the distribution of the main lithological units, including blueschist, greenschist, garnet mica schist, quartz mica schist, and marble, as well as their spatial relationships along the section lines.*

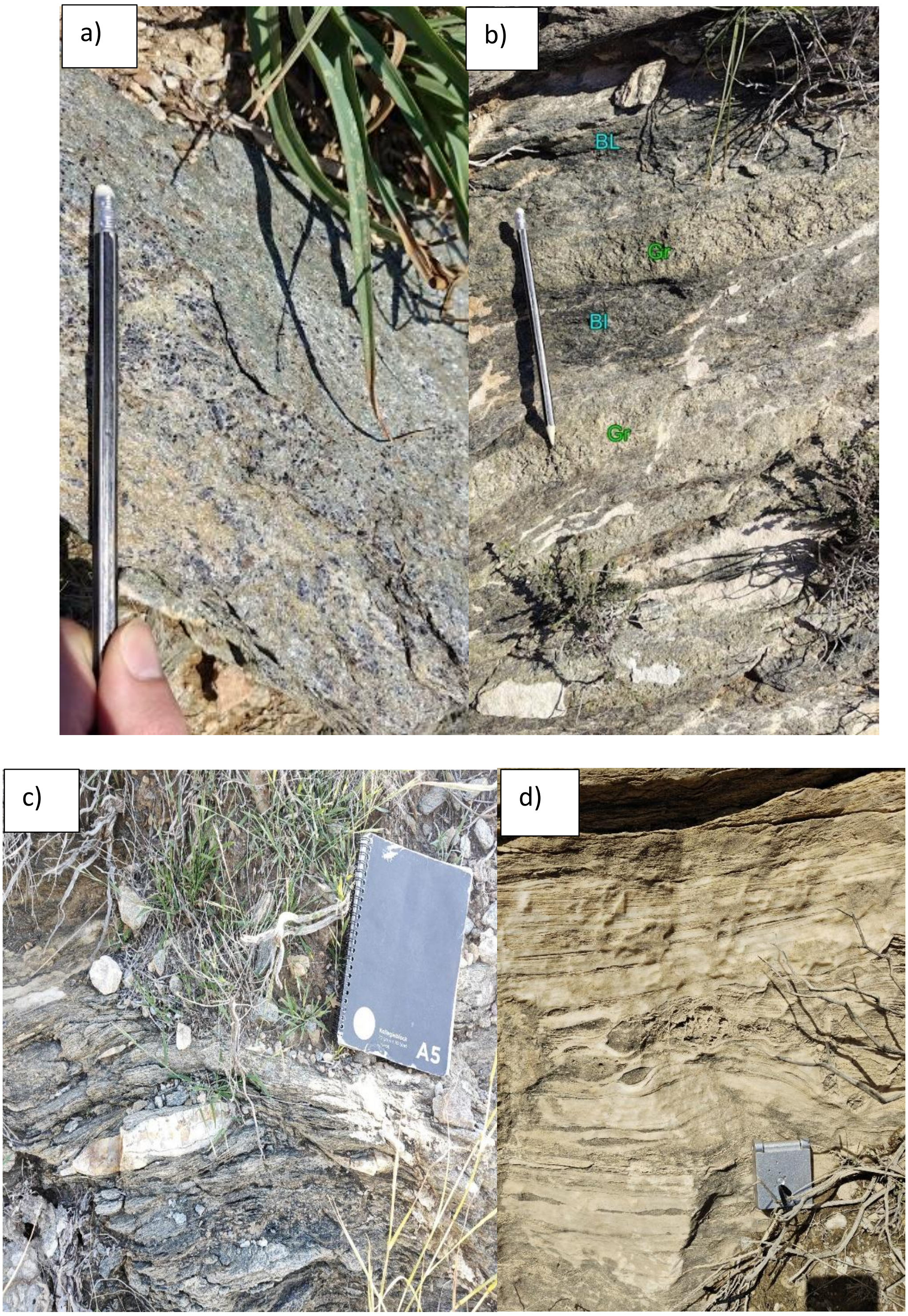

Fig.6 *Examples of rocks found inside the field area: a) Typical blueschist with glaucophane crystals found near Dialiskari Beach b) Greenschist imbricated with blueschist found near Dialiskari Beach c) Quartz mica schist found in the western part of the field area d) Marble found at the contact to mica schist.*

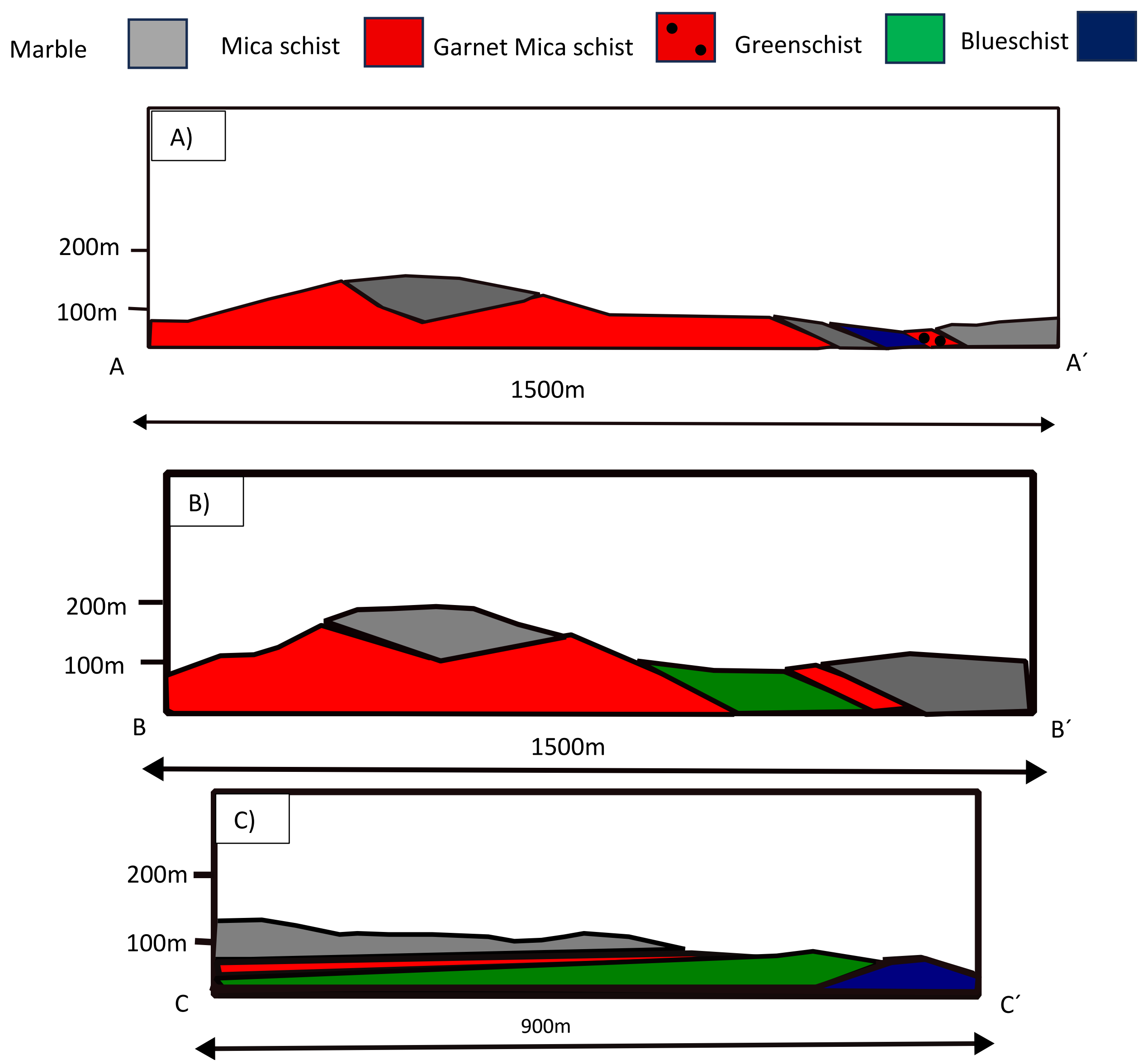

Fig.5 *Cross sections A–A', B–B', and C–C' showing the subsurface lithological relationships inside the field area. The profiles illustrate the distribution and structural arrangement of marble, mica schist, garnet mica schist, greenschist, and blueschist along the section lines.*

4.2 Foliation

Foliation was measured at 186 locations across the study area on exposed rock surfaces, where the planar fabric is defined by the preferred orientation of minerals and structural layering was clearly identifiable.

Foliation measurements are shown on the stereonet as great circles and as poles (Fig. 7). The dataset indicates a predominantly subhorizontal foliation, with 112 out of 186 measurements exhibiting dips toward the northwest and northeast, but the dip is scattered in all directions (Figs. 7 and Table 1). The observed scatter of data points on the stereonet can be attributed to the shallow dip of the foliation. Minor variations in dip angle give rise to substantial differences in dip direction.

Furthermore, the stereonets reveal clustering of dominant dip directions, which vary spatially across the field area depending on the location of measurement. The best-fit great circle to the foliation poles is 30/89 (dip direction/dip); thus, the best-fit fold axis is 301/1 (trend/plunge) (Fig. 7).

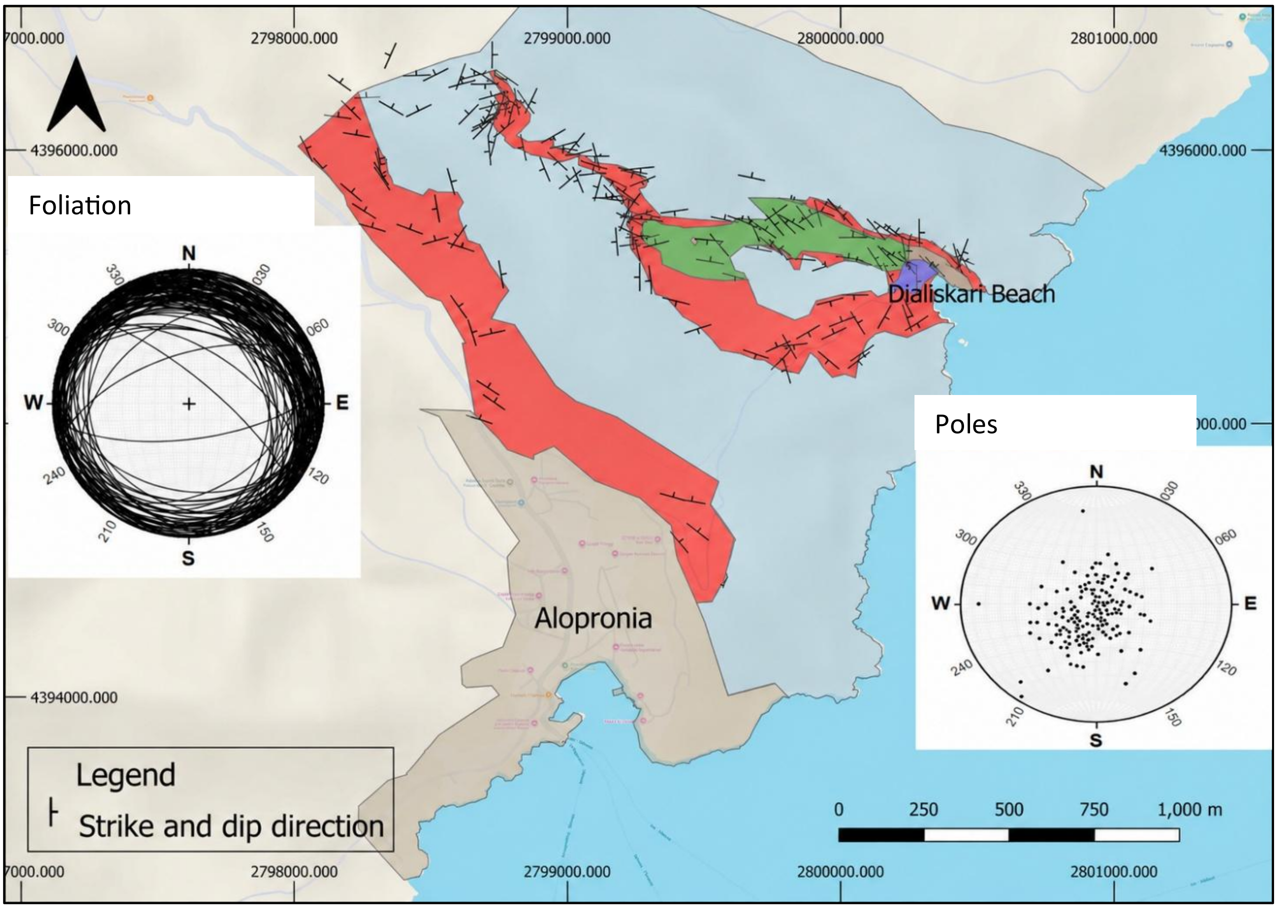

Fig. 7 *A map of the measured 186 dip directions and strikes. The two Stereonets shows the 186 foliation planes and poles. The data from these measurements illustrates a sub horizontal foliation with most measurement dipping towards the northwest or northeast.*

Dip direction	Compass direction	Amount
300–360°	NNW–NW	78
0–60°	NNE–NE	34
60–120°	E–SE	16
120–180°	SE–SSE	14
180–240°	SSW–SW	18
240–300°	W–NW	26

Table.1 *Table of amount of dip direction measurements in compass directions.*

4.3 Stretching lineations

On the foliation planes, well-defined stretching lineations were found. These lineations are expressed by stretched grains of mica, chlorite, quartz, and glaucophane.

The stretching lineation was measured 73 times in the field on the two types of mica schist (29), marble (19), greenschist (15), and blueschist (9) (Fig. 8). The general trend is NNE–SSW, with most measurements close to the stereonet periphery, indicating a low plunge value (Fig. 8). There are some outliers away from the north and south clusters.

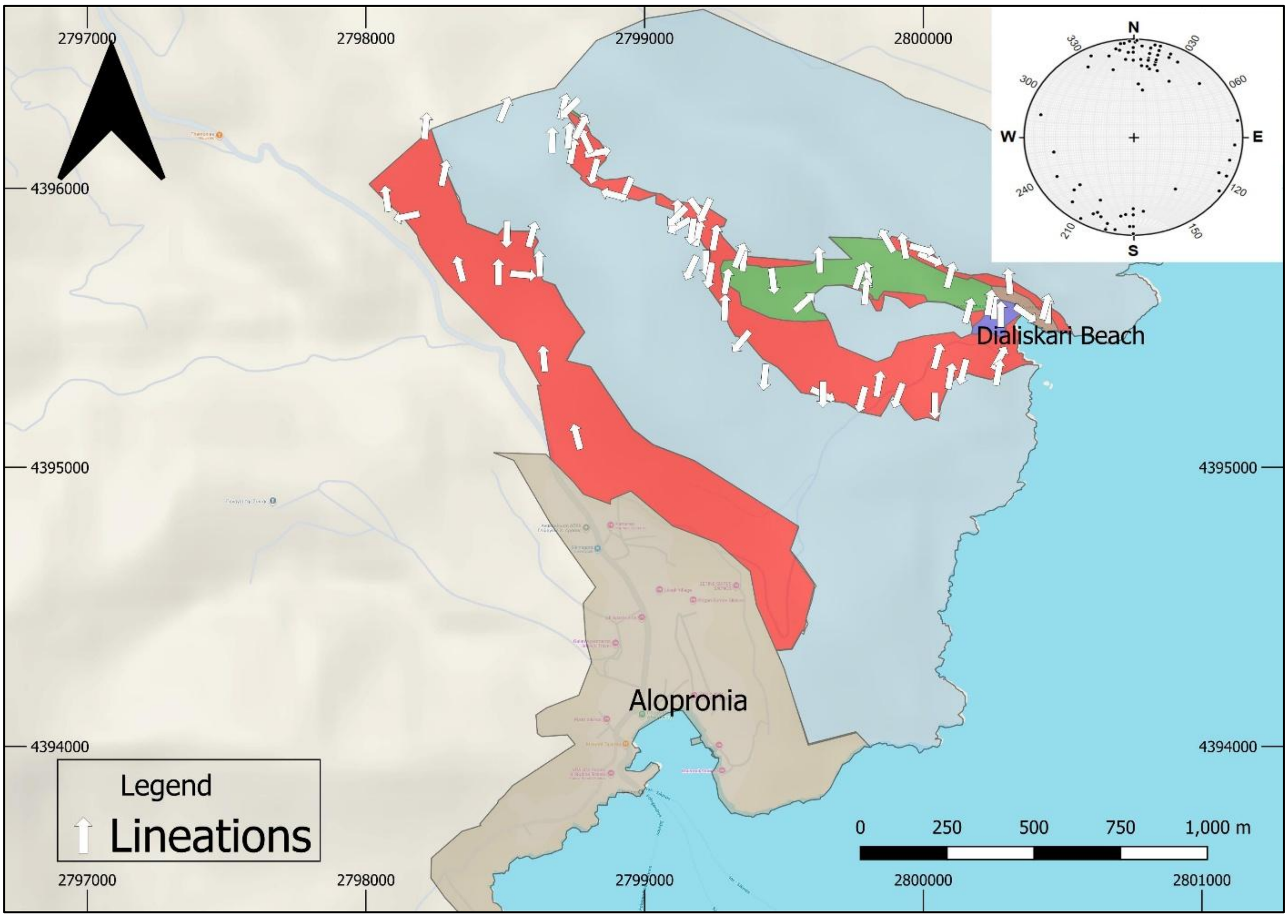

Fig. 8 *Map of stretching lineations. Stereonet in the top right corner shows a general SW-NE tren.*

4.4 Shear sense

The main shear sense documented in the field was top-to-the-S (25 out of 27 measurements) (Fig. 9), with only two locations showing a dominant top-to-the-N sense. Most shear sense indicators were observed in the greenschist-facies mica schist and in the greenschist (24 measurements). The shear sense was interpreted from the strain shadows around garnet porphyroblasts and shear bands (Fig. 10). The clearest shear indicators were identified on the road descending to Dialiskari Beach and in the mica schist to the west. At three locations, high-P garnet mica schist (blueschist facies) was measured. In the garnet, a bidirectional shear sense was documented, but top-to-the-S shear sense dominated.

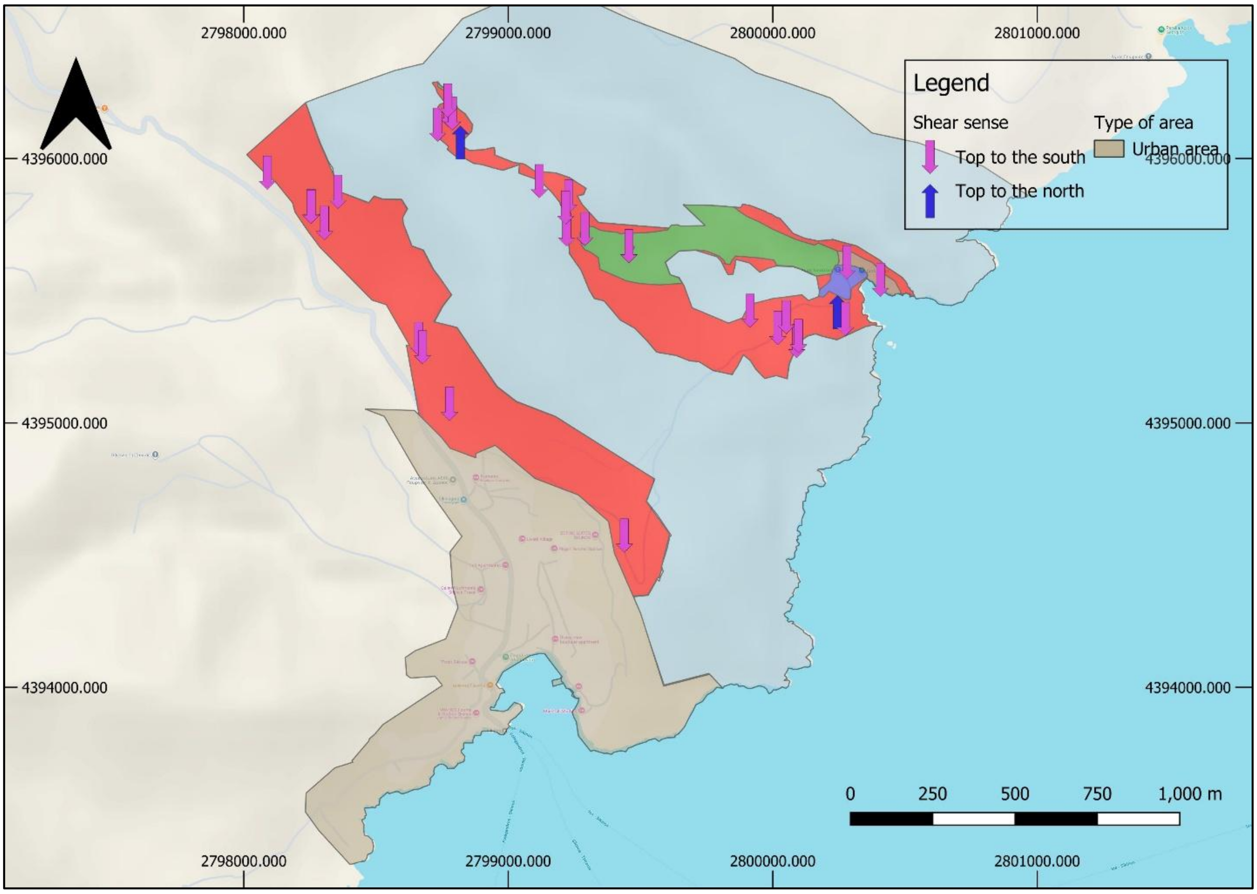

Fig.9 *Map showing the shear sense, purple arrows shows locations with top-to-the-S and blue arrows top-to-the-N.*

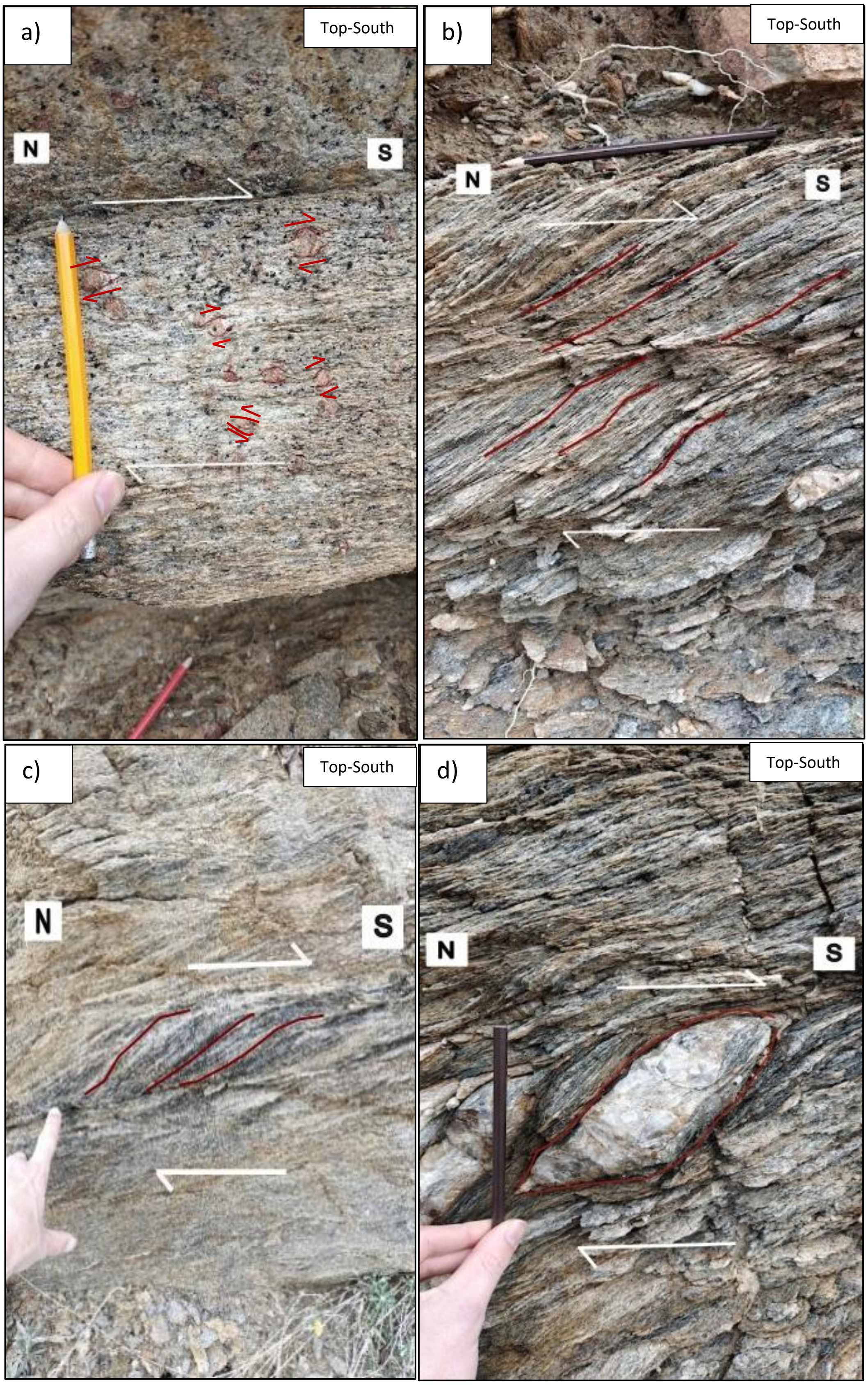

Fig.10 *Examples of shear indicators: a) Garnet porphyroblast with strain shadows showing mainly top-to-the-S GPS: 36°41'12.5"N 25°09'22.4"E b) Shear bands with top-to-the-S shear inside a mica shist GPS:36°41'08.6"N 25°09'11.5"E, c) Shear bands in the mica schist shows top-to-the-S GPS: 36,679834783° N 25,147785617° E, d) Quartz vein inside mica schist with top-to-the-S shear GPS:36°41'08.9"N 25°09'11.9"E*

4.5 Thin section

During fieldwork, four samples, Sik26/4, Sik26/5, Sik26/6, and Sik26/7 were collected for thin sections work. All samples were collected in and around the area of Dialiskari Beach (Fig.10).

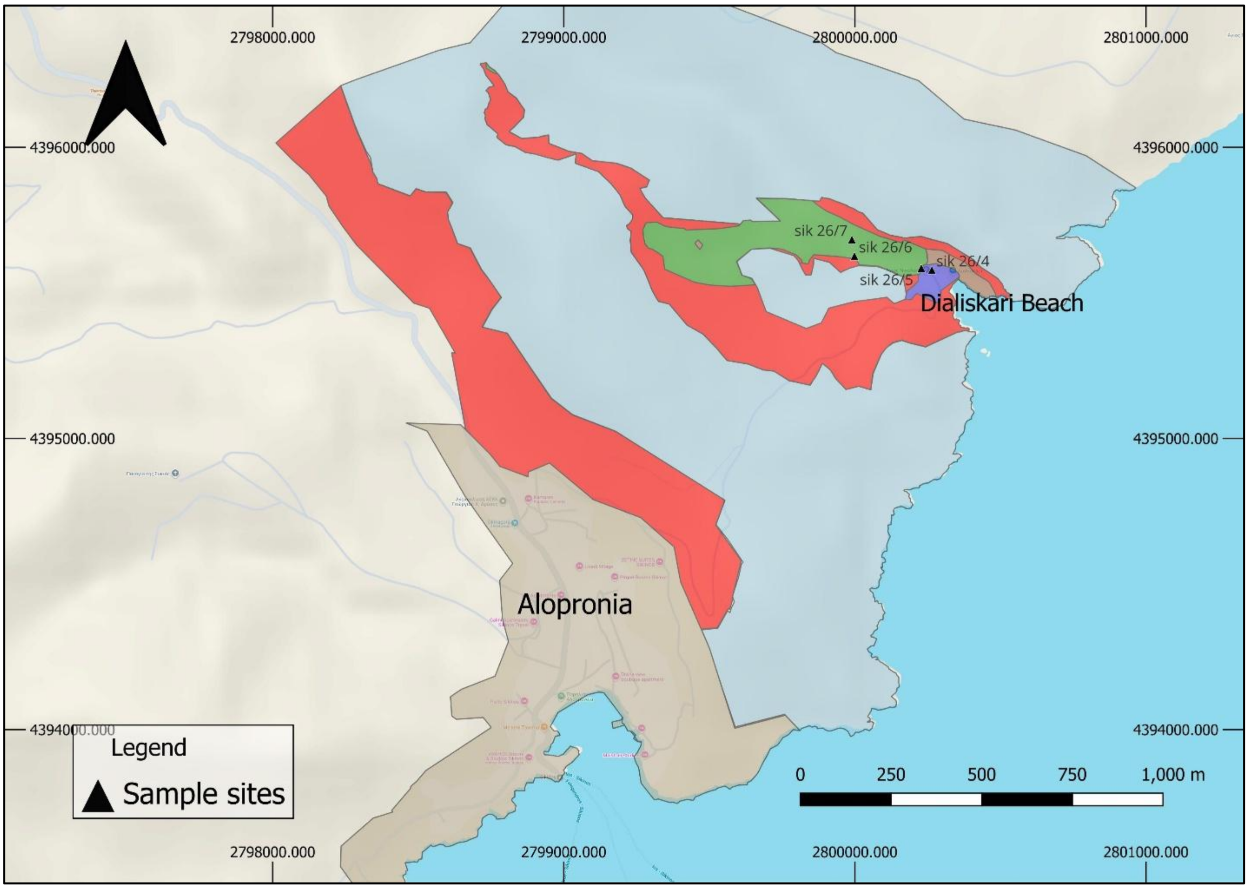

Fig.10 *Map overview of the samples site inside the field area.*

Following annotations were used in the photos of the thin sections (Table.2):

Grt	Garnet	Gln	Glaucophane
Ms	Muscovite	Ep	Epidote
Qz	Quartz	Cal	Calcite
Chl	Chlorite	Op	Opaque minerals
Ab	Albite		

Table 2*: Overview over the abbreviations of common minerals, used in the thin sections below. After* (Whitney and Evans, 2010)

Sample Sik26/4 GPS: (36.6870740830N, 25.1552035500E)

The sample was collected from Dialiskari Beach (Fig. 11), where blueschist has been mapped. The main mineral assemblage in the sample is quartz, glaucophane, albite, and chlorite, with the occurrence of opaque minerals such as pyrite. Textural observations indicate that the glaucophane has undergone retrograde transformation into albite, quartz, and chlorite (Fig. 11). A top-to-the-S shear sense is visible in chlorite shear bands.

Sample Sik26/5 GPS: (36.6871179670N, 25.1548782500E)

The sample was collected at Dialiskari Beach (Fig. 11), at the contact between blue- and greenschist. The main mineral assemblage in the sample is quartz, glaucophane, albite, and chlorite, with a single retrograded garnet present (Fig. 12). Textural observations of both the glaucophane and the garnet indicate replacement by albite, quartz, and chlorite. A top-to-the-S shear sense is visible in the direction of the strain shadows around the retrograded glaucophane.

Sample Sik26/6 GPS: (36.6874179000N, 25.1528149170E)

The sample was collected north of Dialiskari Beach in a stream valley (Fig. 11), at the contact between greenschist and mica schist. The mineral assemblage in the sample is quartz, garnet, albite, chlorite, muscovite, and calcite. Large garnet porphyroblasts are present in the sample (Fig. 12). Textural observations of the garnets indicate replacement by muscovite, quartz, and chlorite. No clear shear sense can be identified.

Sample Sik26/7 GPS: (36.6878281670N, 25.1527349500E)

The sample was collected north of Dialiskari Beach in a stream valley (Fig. 11), within an area where greenschist facies were mapped. The mineral assemblage in the sample is quartz, albite, calcite, glaucophane, and epidote (Fig. 12). Textural observations indicate replacement of the glaucophane indicate by albite, quartz, and chlorite. No clear shear sense can be identified.

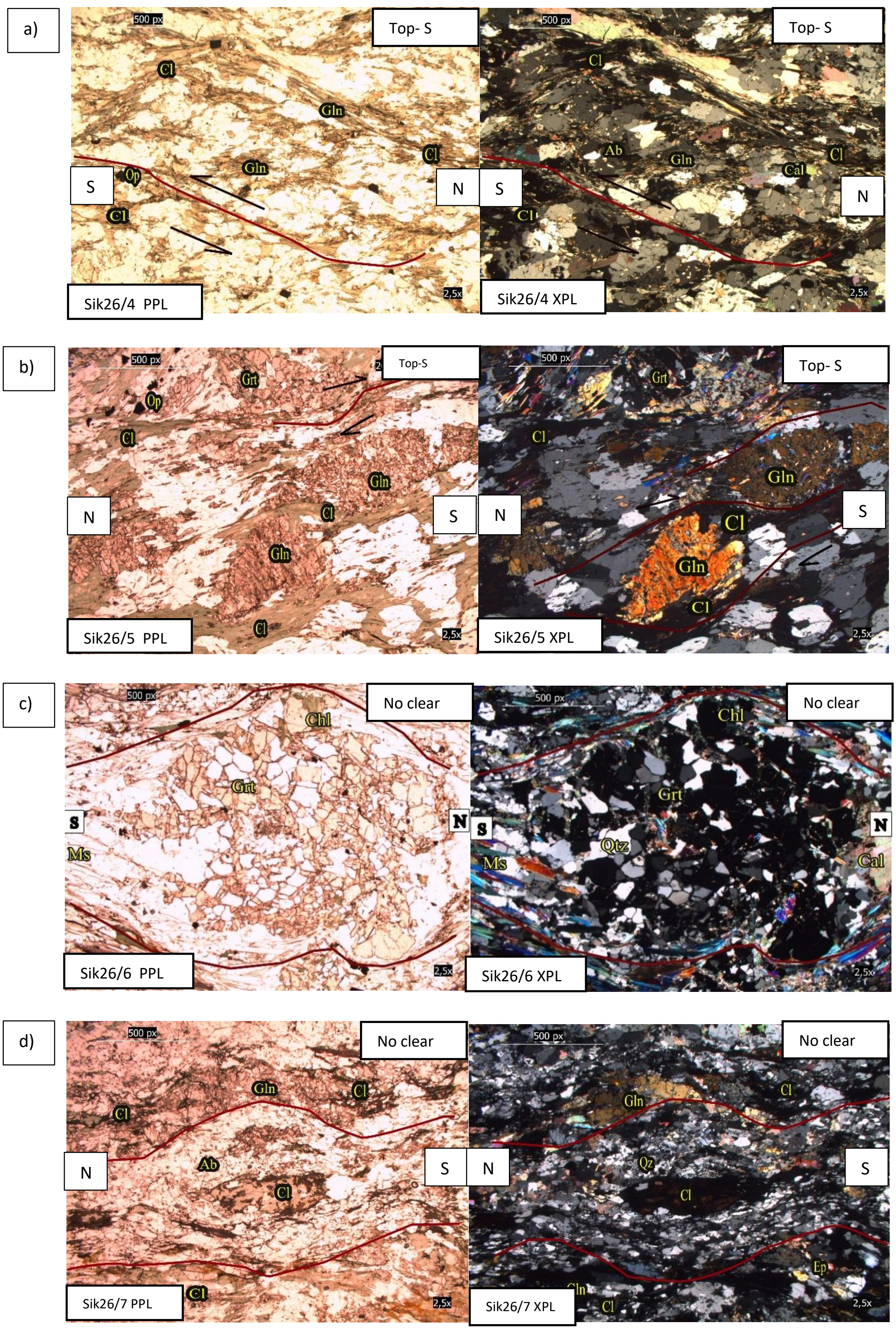

Fig.11 *Microphotographs in PPL and XPL are presented for four samples. (a) Sample Sik26/4 shows glaucophane being replaced by chlorite and albite, with minor occurrences of opaque minerals. The sample also displays chlorite-rich shear bands indicating a top-to-the-S shear sense. (b) Sample Sik26/5 similarly exhibits replacement of glaucophane by chlorite and albite, along with minor opaque minerals, and contains shear bands indicating top-to-the-S shearing. A key difference in (a) is the presence of garnet being replaced by chlorite and muscovite. (c) Sample Sik26/6 contains a large garnet that is being replaced by muscovite, quartz, and chlorite; no clear shear sense could be determined. (d) Sample Sik26/7 shows glaucophane replaced by chlorite, quartz, and albite, and no clear shear sense could be identified.*

5. Discussion

The primary objective of this thesis was to investigate the existence of a shear zone between the 40 Ma blueschist near Agios Georgios Bay and the younger 30 Ma blueschist near Chora. Evidence for such a shear zone is provided by the presence of mylonitic textures, which were observed in most schists during field mapping of the area between the marble units and west of the prominent western marble ridge (Fig. 4).

The foliation and stretching lineations do not contradict the existence of a shear zone. Instead, they are consistent with deformation related to top-to-the-S shearing. The NE–SW clusters of stretching lineations suggest that a force was applied from the NE–SW direction, which corresponds well with the fold axis trend and plunge of 301/1, calculated from the best-fit great circle of the foliation poles. This force may be related to the thrust event around 35–30 Ma, which has been described on the neighbouring island of Ios (Huet, Labrousse and Jolivet, 2009), placing the CBU above the Cycladic Basement (Ring, Glodny and Peillod, 2025).

Clear shear-sense indicators were also identified in the area between the two sample locations, supporting the presence of a shear zone. A dominant top-to-the-S shear sense is observed in greenschist and mica schist (greenschist facies). Top-to-the-S structures are also present in strongly retrograded blueschist, as seen in thin section samples Sik26/4 and Sik26/5 (Fig. 12). Some of these structures appear to have developed during the destabilization of glaucophane and its replacement by chlorite, likely associated with decompression/retrogression. The first top-to-the-S structures developed under blueschist-facies conditions and were progressively overprinted under greenschist-facies conditions during thrusting that placed the CBU above the Cycladic Basement.

To determine the timing of the thrusting of the older blueschist on top of the younger unit, more geochronological data are needed. Additional shear indicators from the blueschist showing top-to-the-S shear would also help strengthen the interpretation.

6. Conclusion

The primary objective of this thesis was to investigate whether a shear zone exists between Agios Georgios Bay and Chora on Sikinos Island. Based on lithological mapping, structural measurements, shear-sense indicators, and thin section observations, the results support the presence of a shear zone in the study area. Within this zone, the rocks are strongly strained and predominantly record a top-to-the-S shear sense. Together with the observed foliation and stretching lineations, this suggests deformation that may be related to thrusting.

7. Acknowledgement

I would like to express my gratitude towards Uwe Ring for all his support during the process of writing this thesis. His contribution ranged from assisting in planning the project, guiding me through the field on Sikinos, providing valuable insights in the writing process and assisting with collecting and obtaining the thin sections. Another thank you should be sent to my colleague Nils Lindström Pettersson, with whom I shared a house with on Sikinos. He and the cat we adopted was a big part of making the time on Sikinos so fun and special.

8. References

Allmendinger, R.W., 2020. Stereonet v.11.

Augier, R. *et al.* (2015) 'Exhumation kinematics of the Cycladic Blueschists unit and back-arc extension, insight from the Southern Cyclades (Sikinos and Folegandros Islands, Greece)', *Tectonics*, 34(1), pp. 152–185. Available at: https://doi.org/10.1002/2014TC003664.

Bakowsky, C. *et al.* (2023) 'Miocene ductile thinning below the Folegandros Detachment System, Cyclades, Greece', *Terra Nova*, 35(3), pp. 220–229. Available at: https://doi.org/10.1111/ter.12646.

Glodny, J. and Ring, U. (2022) 'The Cycladic Blueschist Unit of the Hellenic subduction orogen: Protracted high-pressure metamorphism, decompression and reimbrication of a diachronous nappe stack', *Earth-Science Reviews*, 224, p. 103883. Available at: https://doi.org/10.1016/j.earscirev.2021.103883.

Grasemann, B. *et al.* (2012) 'Miocene bivergent crustal extension in the Aegean: Evidence from the western Cyclades (Greece)', *Lithosphere*, 4(1), pp. 23–39. Available at: https://doi.org/10.1130/L164.1.

Huet, B., Labrousse, L. and Jolivet, L. (2009) 'Thrust or detachment? Exhumation processes in the Aegean: Insight from a field study on Ios (Cyclades, Greece)', *Tectonics*, 28(3). Available at: https://doi.org/10.1029/2008TC002397.

Jolivet, L. *et al.* (2015) 'The geological signature of a slab tear below the Aegean', *Tectonophysics*, 659, pp. 166–182. Available at: https://doi.org/10.1016/j.tecto.2015.08.004.

Jolivet, L. and Brun, J.-P. (2010) 'Cenozoic geodynamic evolution of the Aegean', *International Journal of Earth Sciences*, 99(1), pp. 109–138. Available at: https://doi.org/10.1007/s00531-008-0366-4.

Lister, G.S., Banga, G. and Feenstra, A. (1984) 'Metamorphic core complexes of Cordilleran type in the Cyclades, Aegean Sea, Greece', *Geology*, 12(4), pp. 221–225. Available at: https://doi.org/10.1130/0091-7613(1984)12%3C221:MCCOCT%3E2.0.CO;2.

Meng, J. *et al.* (2021) 'Greece and Turkey Shaken by African tectonic retreat', *Scientific Reports*, 11(1), p. 6486. Available at: https://doi.org/10.1038/s41598-021-86063-y.

Ring, U. *et al.* (2010) 'The Hellenic Subduction System: High-Pressure Metamorphism, Exhumation, Normal Faulting, and Large-Scale Extension', *Annual Review of Earth and Planetary Sciences*, 38(Volume 38, 2010), pp. 45–76. Available at: https://doi.org/10.1146/annurev.earth.050708.170910.

Ring, U. and Glodny, J. (2021) 'Geometry and Kinematics of Bivergent Extension in the Southern Cycladic Archipelago: Constraining an Extensional Hinge Zone on Sikinos Island, Aegean Sea, Greece', *Tectonics*, 40(6), p. e2020TC006641. Available at: https://doi.org/10.1029/2020TC006641.

Ring, U., Glodny, J. and Peillod, A. (2025) 'Top-to-the-S vs top-to-the-N extensional shearing in the southern Cyclades, Aegean Sea, Greece: new geochronologic data', *International Journal of Earth Sciences*, 114(5), pp. 825–840. Available at: https://doi.org/10.1007/s00531-025-02521-2.

Van der Pluijm, B.A. and Marshak, S. (2004) *Earth structure: an introduction to structural geology and tectonics*. Second edition, International student edition. New York: Norton.

Whitney, D.L. and Evans, B.W. (2010) 'Abbreviations for names of rock-forming minerals', *American Mineralogist*, 95(1), pp. 185–187. Available at: https://doi.org/10.2138/am.2010.3371.

Poulaki, E. M., Stockli, D. F., Flansburg, M. E., & Soukis, K. (2019). Zircon U-Pb chronostratigraphy and provenance of the Cycladic Blueschist Unit and the nature of the contact with the Cycladic Basement on Sikinos and Ios Islands, Greece. Tectonics, 38, 3586–3613. https://doi.org/10.1029/2018TC005403